PROGRESS REVIEW • OPEN ACCESS

Reliability of piezoelectric films for MEMS

OPEN ACCESS

Japanese Journal of Applied Physics **62**, SM0802 (2023) **PROGRESS REVIEW**

https://doi.org/**10.35848/1347-4065/acf5f8**

Reliability of piezoelectric films for MEMS

Susan Trolier-McKinstry[1*], Wanlin Zhu[1], Betul Akkopru-Akgun[1], Fan He[1], Song Won Ko[2], Charalampos Fragkiadakis[3], and Peter Mardilovich[3]

[1]*Pennsylvania State University, United States of America*
[2]*Qi2, United States of America*
[3]*aixACCT Systems GmbH, Germany*

[*]E-mail: stmckinstry@psu.edu

Received July 31, 2023; revised August 28, 2023; accepted August 31, 2023; published online September 21, 2023

Thin films based on $PbZr_{1-x}Ti_xO_3$ and $K_{1-x}Na_xNbO_3$ are increasingly being commercialized in piezoelectric MEMS due to the comparatively low drive voltages required relative to bulk actuators, as well as the facile approach to making sensor or actuator arrays. As these materials are incorporated into devices, it is critically important that they operate reliably over the lifetime of the system. This paper discusses some of the factors controlling the electrical and electromechanical reliability of lead zirconate titanate (PZT)-based piezoMEMS films. In particular, it will be shown the gradients in the Zr/Ti ratio through the depth of the films are useful in increasing the lifetime of the films under DC electrical stresses.

1. Introduction

The lifetime of piezoelectric MEMS (piezoMEMS) based on lead zirconate titanate (PZT) under high field bias conditions is important to the performance of these materials as actuators in applications such as adjustable optics, lidar, ink jet print heads, and ultrasound transducers, among others.[1–6)] Over the last several years, the mechanisms responsible for electrical failure have been reported. In many cases, the root cause of failure is associated with the point defect chemistry of the films, which in turn depends on the deposition conditions, as well as changes engendered by subsequent processing.

Figure 1 shows a schematic of the energy band diagram for PZT films. Most undoped PZT films are nearly intrinsic, with weakly *p-type* character in the bulk of the film, and *n-type* character near the electrodes. Donor or acceptor doping is predominantly compensated ionically, with small commensurate changes in the electronic carrier concentration. In most cases, Nb-doping slightly increases the electrical resistivity with respect to undoped films, and acceptor doping (e.g. with Mg, Fe, or Mn on the Zr/Ti site) decreases the electrical resistivity. The process of failure under DC electrical degradation can then be controlled by one of the following factors:

1) The migration of oxygen vacancies induces a decrease in the Schottky barrier height. As this barrier height is reduced, electrical leakage increases, ultimately degrading the insulation resistance.[7–9)] This process is strongly dependent on the initial defect chemistry in the film. Variation in oxygen vacancy concentration through the film thickness leads to voltage polarity dependent lifetime in PZT films. It should be noted that vastly different lifetimes can be observed in films that show comparable values of baseline dielectric and piezoelectric properties. If the electronic charge carrier compensation is spread out over a large volume (further from the electrode interface), for example by a graded doping concentration, the highly accelerated lifetime test (HALT) lifetime can be increased.[10,11)]
2) For films exposed to high relative humidity values, failure can be induced by voltage-induced water splitting, with subsequent migration of oxygen and hydrogen through the electrodes and/or the film.[12)] This failure mechanism can be eliminated with appropriate moisture protection of the MEMS structure.
3) For films with extremely high donor concentrations (e.g. more than approximately 6 mol%), the oxygen vacancy concentration can be low enough that the failure mode changes to one dominated by hole migration.[13)] Akkopru-Akgun reports that lifetimes of the resulting films are slightly lower than optimally doped films with lower Nb concentrations.
4) Electric field-induced cracking can also limit device lifetimes.[14,15)] Many PZT films show a critical tensile stress for cracking that depends on the film thickness with thicker films having lower thresholds for accumulated stress. It is common for thermal failure events to decorate crack pathways; in some cases, these thermal failure events cause additional mechanical failures. The threshold for the mechanical failure depends on the pre-existing population of defects, the ability of the structure to relieve stress by bending, and the built-in stresses associated with the film deposition. PZT films that are prepared in compressive stress states are mechanically significantly more robust than those with a pre-existing tensile stress state. It is easier to electrically induce mechanical failure in films with larger piezoelectric coefficients and breakdown strengths.

For optimized films with a uniform doping profile, the lifetimes can be in the range of 16 h for degradation under accelerating conditions of 200 °C and electric fields of 300 kV cm^{-1}. Given typical activation energies for failure on the order of 0.8–1.25 eV, this produces reasonable lifetimes for piezoMEMS actuators driven at RT and electric fields under 200 kV cm^{-1}. Even higher lifetimes up to 94 h measured under the same conditions can be achieved when graded doping is employed, as mentioned above.[10,11)] It should be

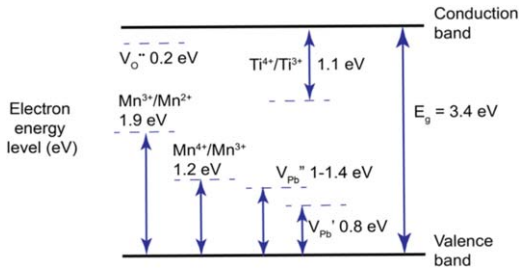

Fig. 1. Schematic of the band structure of PZT films, showing the relative positions of many of the important defect levels.

noted that whereas self-heating is expected to be very modest under DC electric fields, unipolar AC field driving can induce self-heating that could accelerate failure.[16)]

However, there are many factors influencing the PZT film lifetime under DC voltage that are still incompletely understood. In particular, it is noted that many PZT films for piezoMEMS have columnar microstructures. This precludes the possibility of using grain boundaries parallel to the electrodes to serve as barriers to oxygen vacancy or electronic carrier transport, as is ubiquitous in multilayer ceramic capacitors.[17)] This then begs the question as to whether internal barriers within the film can also influence the HALT lifetime.

One possible internal interface that could, in principle, slow the migration of oxygen vacancies, $V_O^{\bullet\bullet}$, is the Zr/Ti gradient characteristic of many chemical solution deposited PZT films. Nucleation of a Ti-rich PZT layer is favored at the bottom of each layer deposited due to the lower nucleation energy; this excludes Zr towards the top of the crystallized layer. Repeated crystallization steps for subsequently deposited layers induce a sawtooth profile for the Zr/Ti ratio through the film depth. Elimination of Zr/Ti gradients of this type increases the film piezoelectric coefficients by moving a larger volume fraction of the film to the morphotropic phase boundary.[18,19)] Pelloquin et al. showed that the RT breakdown strengths were improved in 240 nm thick gradient free films.[20)] Doi et al. suggest that the crystallization interfaces, and potentially the Zr/Ti gradients, suppress the mobility of oxygen vacancies, which can increase lifetime.[21,22)]

There are several potential mechanisms by which this compositional homogeneity might affect the reliability, depending on the deposition conditions. First, the band gap of zirconates exceeds that of titanates,[23)] which might lower the propensity for development of electronic carriers. Secondly, the volatility of PbO increases with the Zr/Ti ratio,[24)] which could induce periodic changes in the defect chemistry through the film depth. Third, the activation energy for formation of V_O^X depends on the Zr/Ti ratio in PZT.[25)] Fourth, any electrical discontinuity could induce p-n junctions that could serve as internal barriers for electromigration of charge carriers to compensate oxygen vacancies. Fifth, Zr is harder to reduce than Ti, which would spread the electron charge compensation layer for electromigrated $V_O^{\bullet\bullet}$ over larger depths, which in turn might reduce the propensity for Schottky barrier lowering, and hence increase the lifetime for degradation when the cathode side is Zr-rich.

However, it is not known which, if any, of these factors matters, or to what extent. Thus, the purpose of this paper is to examine the role of Zr/Ti gradients in controlling the HALT lifetime under DC electric fields for PZT films for piezoMEMS applications.

2. Experimental procedure

Chemical solution derived graded and gradient free PZT films with an average composition at the morphotropic phase boundary (e.g. Zr/Ti ratio of 52/48 with 2% Nb on the Zr/Ti site) were prepared. The substrates used were Pt-coated Si wafers in which the Pt was deposited at RT, producing Pt {111} rocking curves full width at half maximum of ~4.7°. Solutions were purchased from Mitsubishi Materials Corporation. {100} orientation for the PZT films was seeded as previously reported using a Pb and Ti-rich PZT layer, such that the Pb/Nb/Zr/Ti ratio in the solution was 120/2/44/56.[26)] In brief, films with Zr/Ti gradients were prepared using a single PZT solution for the bulk of the film with a Pb/Nb/Zr/Ti ratio in the solution of 114/2/52/48. Gradient free samples were prepared using multiple solutions to counteract the tendency for compositional segregation (e.g. the first layer in a sequence had a solution Zr/Ti ratio of 60/40, the second 52/48, and the third 44/56). The films were pyrolyzed after each spin coating step, and crystallized after every three spin-coated layers, as reported elsewhere.[26)] Aside from this, the processing of the graded and gradient free films was otherwise identical. In both cases, the spin-coating, pyrolysis and crystallization steps were repeated until a thickness of 1.5–2 μm was achieved; the thickness of the layer crystallized in a single step was 200 ± 10 nm in both cases. Some of the samples were released from the substrate by deep reactive ion etching (DRIE) to create diaphragms; others were left clamped to the substrate. The top electrodes for the samples which were released were IrO_2/Ir, whereas the top electrodes for the clamped samples were Pt.

DC leakage current measurements were made using a Keysight 4140B picoammeter. The voltage was increased in 1 V increments. The voltage was held for 60 s to allow transient polarization currents to decay before measuring the steady-state leakage current. Then, the voltage was increased progressively until a field of 600 kV cm^{-1} was reached.

HALTs were conducted using DC fields of 300 kV cm^{-1} and an accelerating temperature of 200 °C to ensure the transport and subsequent accumulation of oxygen vacancies near the cathode Pt/PZT film interface. 12 identical capacitors were tested simultaneously to develop some statistical significance for the results. For both gradient and gradient free films, HALT tests were conducted on separate samples so that the polarity-dependence of the lifetime could be assessed using 0.04646 mm^2 electrodes.

Thermally stimulated depolarization current (TSDC) measurements were made as reported previously,[9)] using 3 mm diameter top electrodes on clamped samples. Samples were degraded under 80, 100, or 120 kV cm^{-1} at 160 °C for 6 h, and then cooled down to RT under an electric field. All trapped charges, defect dipoles, and space charges are frozen in this state. The electric field was subsequently removed, and the sample was short circuited to monitor depolarization current while the sample was heated at a constant heating rate from 40 °C to 350 °C. To explore the physical origin of TSDC peaks, the dependence of T_{max} on degradation electric field was studied. Heating rates of 6, 8, and 10 °C min^{-1} were utilized to extract the activation energies for different depolarization peaks using the heating rate method.[9)]

Modulus measurements were made on clamped gradient and gradient free samples at temperatures from 280 °C–400 °C for frequencies of 0.1 to 10^5 Hz using a Solartron SI1287 electrochemical interface and 1255B frequency response analyzer. The activation energies for the conduction were extracted from the temperature dependence of the fitted modulus peak.

Laser interferometry measurements were made on gradient and gradient free diaphragm samples. The displacement was measured at increasing electric fields, up to 200 kV cm^{-1} at approximately quasi-static conditions (100 Hz, whereas the fundamental resonance frequency of these devices was 2.4 MHz) and at RT (25 °C), using an AixACCT PES and TFAnalyzer 3000 system.[16)]

3. Results and discussion

Figure 2(a) shows the X-ray diffraction patterns for graded and gradient free PZT films. Both films were phase pure within the detection limits of the tool, and both strong levels of {100} texture. Neither film shows clear evidence for significant tetragonal splitting of the {200} peak.

As shown in Fig. 2(d), the use of multiple solutions to reduce the Zr/Ti gradients was successful in reducing the sawtooth profile for the Zr/Ti ratio (the apparent reduction in the composition swings through the depth of the film are an artifact of the intermixing that occurs during the milling). Figures 2(e) and 2(f) shows FESEM cross-sections of the films. In both gradient and gradient free films, the microstructures are columnar. The faint horizontal lines every ∼200 nm thickness correspond to individual crystallization steps.

Table I shows a comparison of the baseline electrical properties of the gradient and gradient free PZT films. As expected from the literature, the gradient free film shows a higher relative permittivity of ∼1470 at 1 kHz, whereas the sample with the Zr/Ti gradient has a permittivity of ∼1280. In both cases, the loss tangents were around 3.5%. Both sets of films had high breakdown strengths of 800 kV cm^{-1} at RT.

To assess the asymmetry of the conduction mechanisms, leakage current data were measured for both polarities in the graded and gradient free films, as shown in Fig. 3(a). For both polarities, it is clear that the gradient free samples had slightly lower leakage current densities for a given field. The slightly higher leakage current for the field down direction for both sets of films would be consistent with the asymmetry in the top and bottom electrodes. Intriguingly, lower leakage

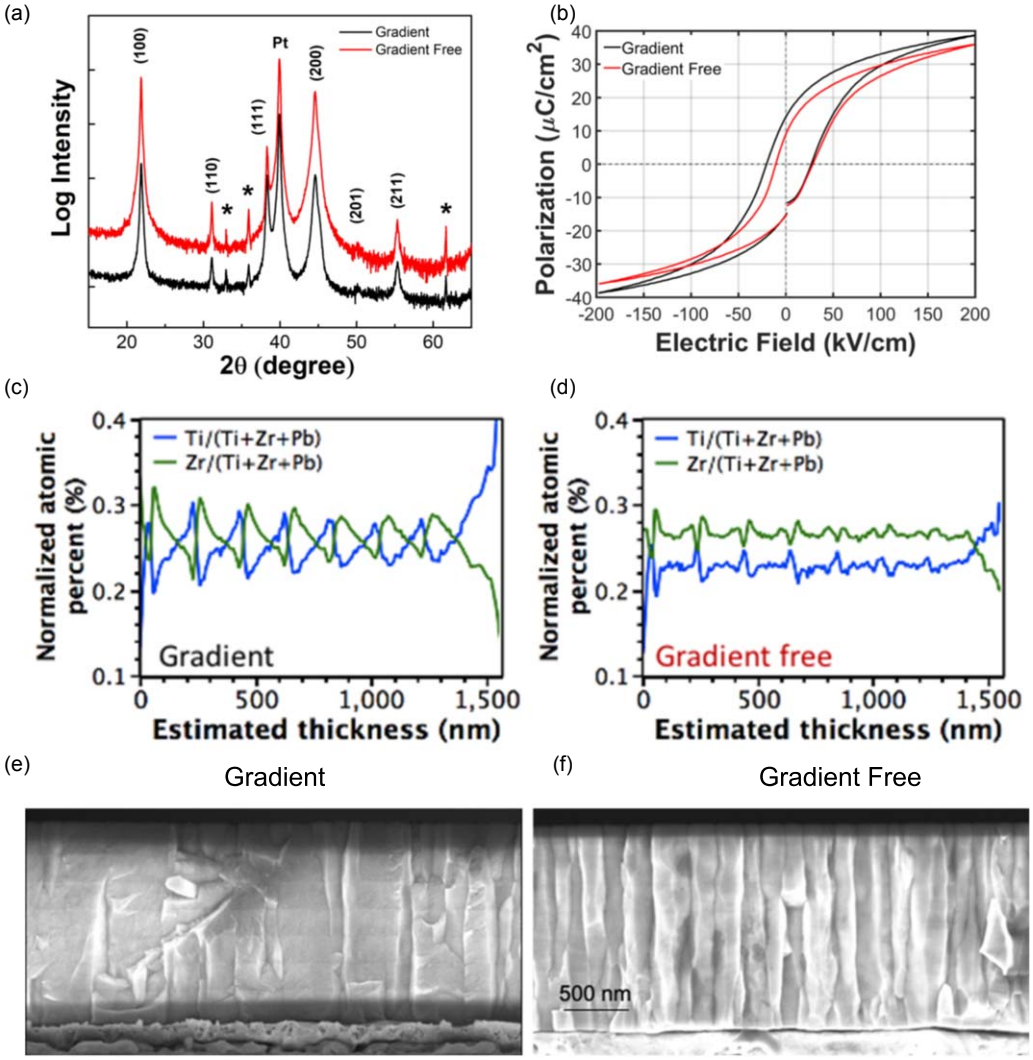

Fig. 2. Comparison of graded and gradient free films. (a) X-ray diffraction patterns showing comparable crystallinity and strong {100} orientation. The starred peaks are from the substrates or from other X-ray wavelengths, such as Cu K_β, (b) Polarization—electric field hysteresis loops, (c), (d) compositional depth profiles, and (e), (f) scanning electron micrographs of film cross sections.

Table I. Comparison of gradient and gradient free PZT films. ε_r is relative permittivity, P_r is remanent polarization, E_c is coercive field, E_i is imprint and E_B is electrical breakdown field. The imprint was measured after poling either field up or field down at 200 kV cm^{-1} for 30 min at 150 °C. The polarization measurements were performed by driving the bottom electrode and the observed positive shift of the polarization loop indicated an initial field down imprint in both films, albeit more pronounced in the gradient free case.

	ε_r	Tanδ	P_{r-}, P_{r+} (μC cm^{-2})	E_{c-}, E_{c+} (kV cm^{-1})	E_i initial and after poling field down/up (kV cm^{-1})	E_B field down/up (kV cm^{-1})
Gradient	1280	0.033	−15.3, 14.1	−20.3, 27.0	3.33, 9.43/ −7.73	793/830
Gradient free	1470	0.035	−15.5, 9.0	−10.5, 28.5	8.9, 13.2/ −3.25	785/818

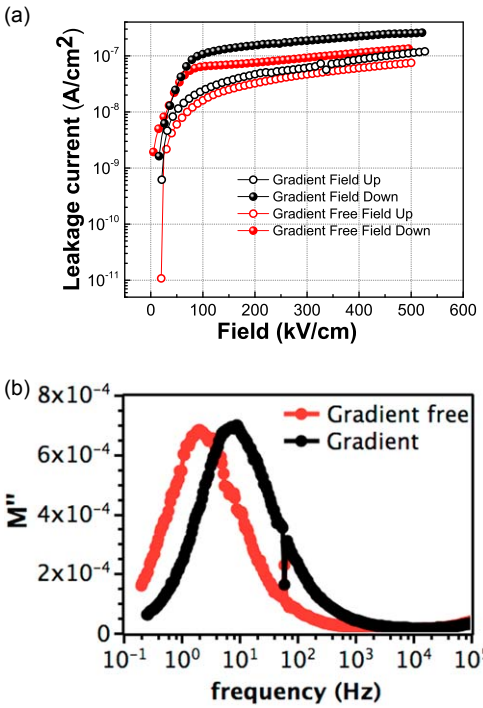

Fig. 3. (a) Leakage current densities for the graded and gradient free PZT films measured for both field polarities on released samples with IrO_2/Ir top electrodes (b) Modulus spectroscopy data for graded and gradient free PZT films measured at 320 °C.

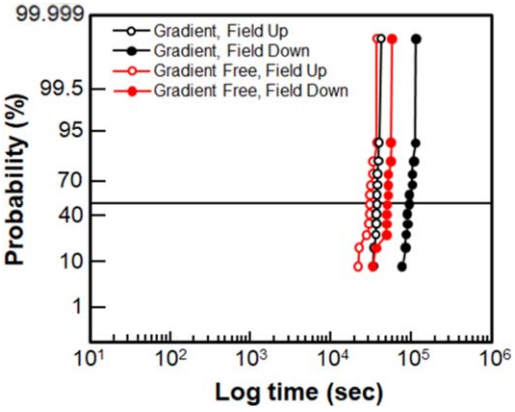

Fig. 4. Probability of failure as a function of time under HALT measurement conditions of 300 kV cm^{-1}, 200 °C for PZT with and without Zr/Ti gradients measured with field up and field down directions.

current levels were observed at the IrO_2/PZT interface despite its lower work function compared to the Pt electrode. This suggests that the barrier height is in between the Schottky and Bardeen limits, where it is not only controlled by work function of electrode but also by the presence of defect sites, such as oxygen vacancies, near the interface that lower the barrier height through Fermi level pinning.[27,28] This effect would be expected to be less severe near the IrO_2/PZT interface since oxide electrodes can act as an oxygen source, reducing the oxygen vacancy concentration at this interface.

To minimize the effect of the electrode asymmetry, modulus spectroscopy measurements were conducted on gradient and gradient free samples with Pt top electrodes [see Fig. 3(b)]. The higher frequency for the modulus peak of the sample with Zr/Ti gradients is consistent with the leakage current data in Fig. 3(a), e.g. that the films with a Zr/Ti gradient are also more electrically leaky. The modulus peaks were fitted for data collected between 280 °C and 400 °C, and were utilized to extract the activation energy for conduction for both types of samples. It was found that films with and without Zr/Ti gradients had activation energies for conduction of 1.2 ± 0.1 eV;[29] this activation energy is consistent with Ti^{3+}/Ti^{4+} electron hopping at these temperatures. This identical activation energy suggests that the electronic conduction mechanism for the graded and gradient free samples is the same.

It is speculated that the higher conductivities for the films with the gradients may be associated with a higher defect concentration built in during the film synthesis. It is noted that the volatility of PbO is higher from $PbZrO_3$-rich PZT than from $PbTiO_3$-rich PZT.[24] Thus, the top surfaces of the films with a Zr/Ti gradient are more susceptible to PbO loss. The resulting higher concentration of traps in the films for electrons and holes could induce the higher conductivity.

Figure 4 shows the HALT lifetimes measured under the same conditions for films with and without Zr/Ti gradients associated with compositional segregation during the crystallization of a chemical solution-derived PZT film. Measurements were made for DC fields of 300 kV cm^{-1} at 200 °C on released samples with IrO_2/Ir top electrodes. It is apparent that for degradation in either voltage polarity, the lifetime is higher for the film with the Zr/Ti gradients. For the field up measurement conditions, the median time to failure, t_{50}, is 10.64 h, relative to the gradient free t_{50} of 8.64 h. For field down, t_{50} is 26.69 h for the graded film and 14.16 h for the gradient free film. Thus, for both polarities, the existence of the Zr/Ti gradients *increases* the lifetime of these films, with the higher lifetimes observed in the field down configuration, for which charge injection would occur through the Pt, rather than the IrO_2 electrode.

It is notable that these results differ from the reports from Doi et al.,[21,22] who reported higher lifetimes in gradient free samples. In that work, however, the data are convoluted with a substantial change in grain size of the gradient and gradient free samples which was not observed here. It is possible that is the origin of the discrepancy.

The higher HALT lifetimes in the field-down direction are correlated with a higher leakage current in the same direction.

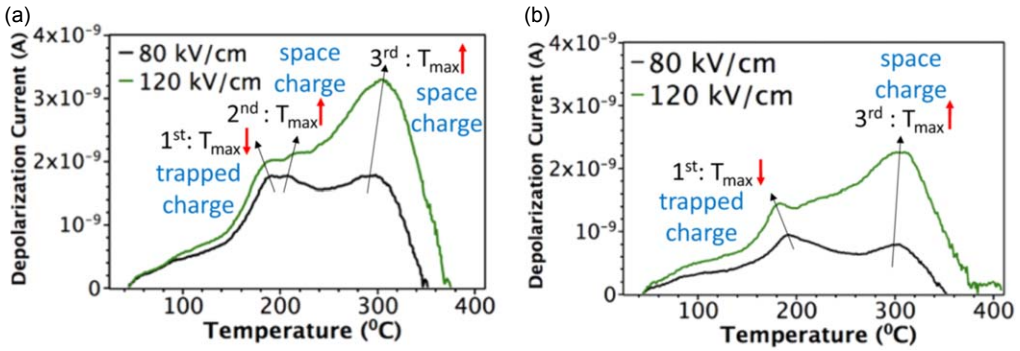

Fig. 5. TSDC spectra of (a) gradient and (b) gradient free films after electrical degradation at 80 and 120 kV cm^{-1} at 160 °C for 6 h.

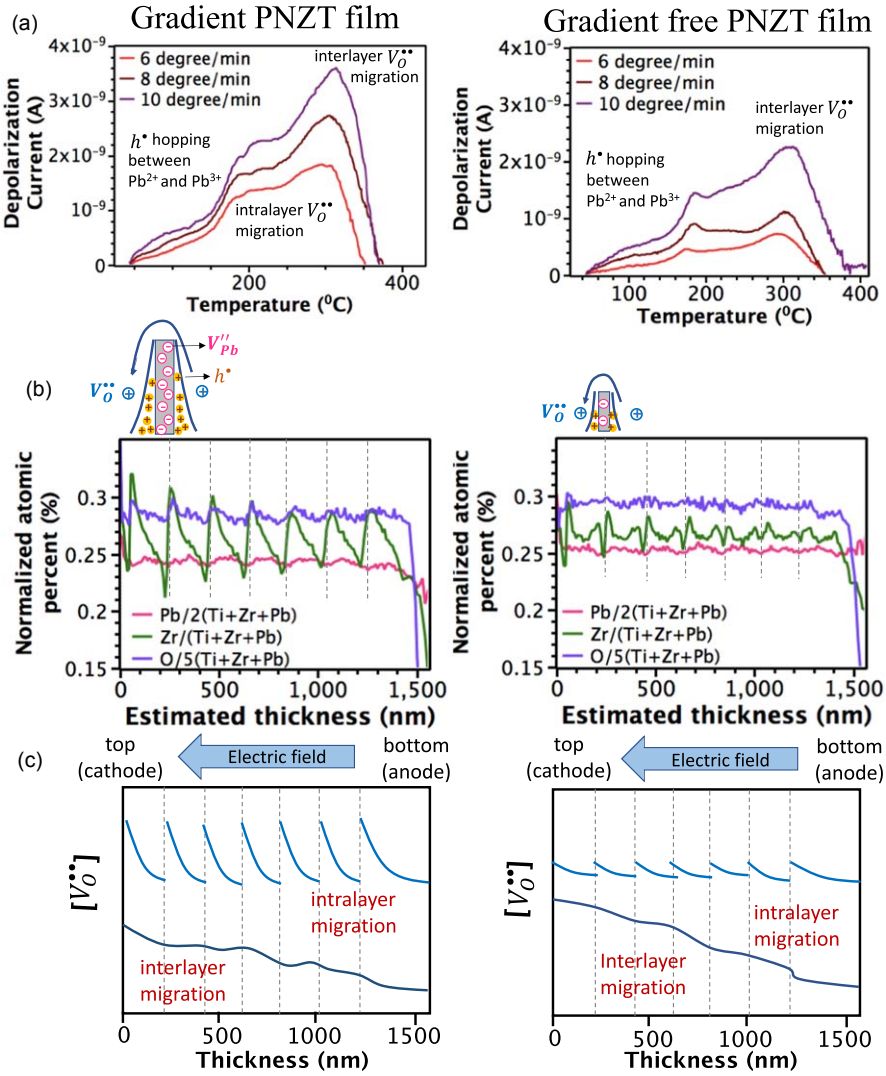

Fig. 6. (a) TSDC spectra collected at different heating rates, (b) XPS depth profiling, and (c) Schematic representation of intra and interlayer oxygen migration in gradient and gradient free films.

The leakage currents measured in this work are expected to be dominated by electron or hole transport, whereas the HALT lifetimes are likely to be controlled by the transport of oxygen vacancies at higher temperatures for longer times. This difference in the species controlling the behavior is likely to be the origin of the observation that the higher leakage current direction is associated with the higher HALT lifetime. It is speculated that the Zr/Ti gradients act as additional blocking layers for ion transport.

To assess the validity of this speculation, TSDC were collected on samples with Pt top and bottom electrodes, with and without Zr/Ti gradients. As shown in Fig. 5, three TSDC peaks were observed for gradient films. The electric field dependence of peak temperature was studied to explore the depolarization mechanism. The 1st (low temperature) peak shifted toward lower temperature with increasing polarizing electric field, E_p, suggesting that it originates from trapped charges. Both the 2nd (intermediate temperature) and 3rd

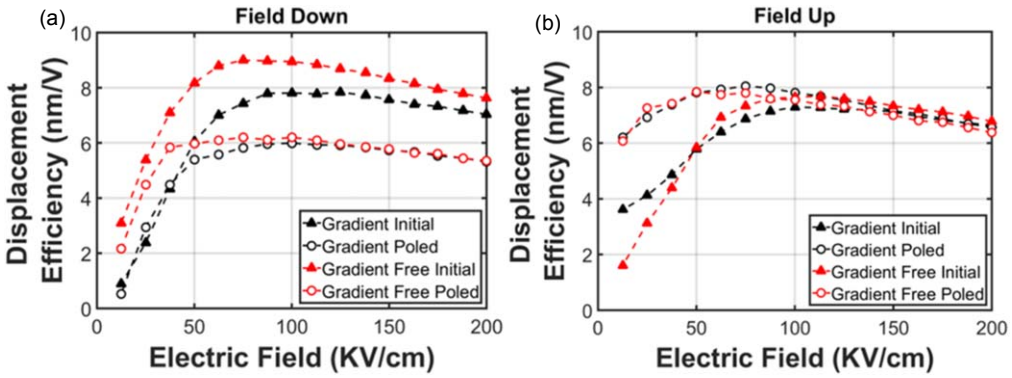

Fig. 7. Plots of the initial and after poling displacement efficiency (displacement/voltage) as a function of electric field for actuators made with gradient and gradient free PZT on thin flexible diaphragms. Field Down operation (a) and field Up (b).

(high temperature) TSDC peaks moved to higher temperatures with increasing E_p, indicating that they are due to depolarization of space charges.

The heating rate method was used to estimate activation energies of the TSDC peaks [Fig. 6(a)]. The trapped charge peak has an activation energy of 0.38 ± 0.1 eV, attributed to hole hopping between Pb^{2+} and Pb^{3+}.[29] The intermediate and high temperature space charge peaks, on the other hand, have activation energies of 1.1 ± 0.1 and 0.7 ± 0.1 eV, which could be associated with oxygen migration within and between crystallization layers, respectively.[7,9] A similar trapped charge peak was also observed for gradient free films. Intriguingly, only one space charge peak attributed to long-range migration of oxygen vacancies was detected for these films, implying that Ti/Zr gradient might act as a blocking layer for oxygen vacancy migration. Figure 6(b) shows the variation in relative atomic percentages of Pb, Zr, and O through the depth of the film, as measured by XPS. In gradient films, at the surface of each layer, the film becomes Zr rich and lead loss upon crystallization is increased in these regions. There is also oxygen enrichment at the surface of each crystallized layer, indicating that superoxidation occurs through absorption of oxygen from the atmosphere [Eq. (1)].[30] This makes the surface of each layer more p-type.

$$\frac{1}{2}O_2(g) \rightarrow V''_{Pb} + 2h^{\bullet} + O_O \qquad (1)$$

Together with holes, V''_{Pb} create space charge at the surface of each layer that might hinder $V_O^{\bullet\bullet}$ migration between the layers. This effect is more pronounced in Ti/Zr gradient films due to propensity for V''_{Pb} formation in Zr-rich regions [Fig. 6(b)]. Figure 6(c) is a schematic representation of oxygen vacancy migration in gradient and gradient free films. Under an applied electric field, $V_O^{\bullet\bullet}$ migrate and subsequently accumulate at the surface of each crystallization layer in gradient films. This additional barrier for ion transport might delay long-range oxygen vacancy migration through the thickness of the film, and subsequent buildup near the cathode interface. This can prevent severe Schottky barrier lowering and improves lifetime. For gradient free films, on the other hand, the lack of a barrier for oxygen vacancy migration at each crystallization surface can enhance long-range oxygen vacancy migration, leading to higher leakage current rise upon electrical degradation and lower lifetime.

In addition to understanding the lifetime, it is also useful to probe how Zr/Ti gradients influence the performance of piezoMEMS actuators. The devices were fabricated from the same type of wafers described above, when the Si was etched from the backside using DRIE. Details of those actuators can be found elsewhere.[16] The displacement was measured in both polarities, when the electrical field was applied down, in the direction of the internal field, and when the electric field was applied up, from bottom electrode to the top. The PNZT was poled at 200 kV cm^{-1} for 30 min at 150 °C in both directions. After poling field down, the E_i was changed from 3.33 to 9.43 kV cm^{-1} and from 8.9 to 13.2 kV cm^{-1} for graded and gradient free PNZT respectively. By poling in the field up direction, the internal field was shifted from field down to field up (Table I).

Figure 7 shows the displacement efficiency (displacement of the actuator per 1 volt) for actuators made from graded and gradient free PNZT as received (e.g. the initial performance), and after poling. Figure 7(a) shows that for field down driving, the gradient free actuator (e.g. driving in the direction of the internal field), performs better than the graded one, which is consistent with Refs. 18, 21. Not surprisingly, after poling in the same direction, the displacement efficiency decreases; the drop is substantially larger for the actuator with gradient free PNZT, from approximately 9–6 nm V^{-1}. Moreover, after poling the displacement efficiency of gradient free PNZT is just slightly better than that of the graded actuator, and only at electric fields below 75 kV cm^{-1}. The poling procedure is not much different from applying an electric field for a very long time at operating temperatures, as is expected from PZT based piezoMEMS devices. As an example, if the actuator operates in the field down direction, its performance will degrade in time and stabilize around the efficiency that can be reached much faster through the poling procedure. Thus, the most practical displacement efficiency is not the initial one but rather the one after poling.

In the field up direction, the actuators behave differently. The gradient free actuator has slightly better performance when the applied electric field exceeds 50 kV cm^{-1}, but after poling field up the difference in the performance of graded and gradient free PNZT is diminished. Both their displacement efficiencies are around 8 nm V^{-1} at ∼75 kV cm^{-1}, compared with ∼6 nm V^{-1} when poling was performed field down.

It should also be noted that the most significant increase of the performance of the actuators after poling is when the PNZT is used in field up direction and the electrical field is below 75 kV cm^{-1}. In some applications thin film actuators are utilized at even lower electrical fields. This may be the regime for which gradient free films are most useful.

As shown above (Fig. 4), the probability of failure is lower with field down operation, and it is lower for graded PNZT. Whether the higher lifetime is critical in applications will depend on the details of the system and the duty cycle. For the films described here, the higher displacement efficiency of the gradient free actuator may enable lower voltages than would be necessitated in the actuators with the Zr/Ti gradients. Decreasing the operation voltage will improve the reliability of the device, decreasing the probability of failure.

4. Conclusions

A series of PZT films with average compositions at the morphotropic phase boundary, with and without Zr/Ti gradients were prepared using chemical solution deposition. It was found that the films with the Zr/Ti gradient had a higher point defect concentration as prepared, which produced slightly higher leakage current densities. Nonetheless, it is found that Zr/Ti gradients in PZT films increase the lifetime under DC electric fields. It is speculated that the sawtooth profile gradients associated with multiple crystallization steps in CSD films act as barriers for $V_O^{\bullet\bullet}$ migration. There is a clear advantage to the use of gradient free films in sensor and energy harvesting applications in which the films are poled once, and then are not exposed to high electric fields during use. Actuators made with gradient free films had higher displacement efficiencies at low electric fields ($<$100 kV cm^{-1}) which may allow use of the higher piezoelectric performance without a reliability penalty in devices which can be driven at low electric fields. In applications which require higher electric field drive, however, the higher reliability of the films with Zr/Ti gradients is advantageous.

Acknowledgments

This work is supported through the National Science Foundation (IIP-1841466 and IIP-1841453) and the Center for Dielectrics and Piezoelectrics.
The authors wish to thank XAAR plc for allowing the authors to use their test dies in this study.

1) J. Thorstensen, J. T. Thielemann, P. Risholm, J. Gjessing, R. Dahl-Hansen, and J. Tschudi, "High-quality dense 3D point clouds with active stereo and a miniaturizable interferometric pattern projector," Opt. Express **29**, 41081 (2021).
2) C. Y. Cheng et al., "Thin Film PZT-Based PMUT arrays for deterministic particle manipulation," IEEE Trans. Ultrason. Ferroelectr. Freq. Control **66**, 1606 (2019).
3) (https://fujifilm.com/us/en/business/inkjet-solutions).
4) R. R. Benoit, R. Q. Rudy, J. S. Pulskamp, and R. G. Polcawich, "Piezoelectric RF MEMS switches on Si-on-sapphire substrates," J. MEMS **29**, 1087 (2020).
5) Y.-Q. Qiu, J. Gigliotti, M. Wallace, F. Griggio, C. Demore, S. Cochran, and S. Trolier-McKinstry, "Piezoelectric micromachined ultrasound transducer (PMUT) arrays for integrated sensing, actuation, and imaging," Sensors **15**, 8020 (2015).
6) S. Trolier-McKinstry and P. Muralt, "Thin film piezoelectrics for MEMS," J. Electroceram. **12**, 7 (2004).
7) B. Akkopru-Akgun, T. Bayer, K. Tsuji, C. A. Randall, M. T. Lanagan, and S. Trolier-McKinstry, "Leakage current characteristics and DC resistance degradation mechanisms in Nb doped PZT films," J. Appl. Phys. **129**, 174102 (2021).
8) B. Akkopru-Akgun, T. Bayer, K. Tsuji, C. A. Randall, M. T. Lanagan, and S. Trolier-McKinstry, "The influence of Mn doping on the leakage current mechanisms and resistance degradation behavior in lead zirconate titanate films," Acta Mater. **208**, 116680 (2021).
9) B. Akkopru-Akgun, D. M. Marincel, K. Tsuji, T. Bayer, C. A. Randall, M. T. Lanagan, and S. Trolier-McKinstry, "Thermally stimulated depolarization current measurements on degraded lead zirconate titanate films," J. Am. Ceram. Soc. **104**, 5270 (2021).
10) W. Zhu, B. Akkopru-Akgun, J. I. Yang, C. Fragkiadakis, K. Wang, S. Won Ko, P. Mardilovich, and S. Trolier-McKinstry, "Influence of graded doping on the long-term reliability of Nb-doped lead zirconate titanate films," Acta Mater. **219**, 117251 (2021).
11) D. Koh, S. Won Ko, J. In Yang, B. Akkopru-Akgun, and S. Trolier-McKinstry, "Effect of Mg-doping and Fe-doping in lead zirconate titanate (PZT) thin films on electrical reliability," J. Appl. Phys. **132**, 174101 (2022).
12) R. P. Dahl-Hansen, J. Marc Polfus, E. Vøllestad, B. Akkopru-Akgun, L. Denis, K. Coleman, F. Tyholdt, S. Trolier-McKinstry, and T. Tybell, "Electrochemically driven degradation of chemical solution deposited ferroelectric thin-films in humid ambient," J. Appl. Phys. **127**, 244101 (2020).
13) B. Akkopru-Akgun, K. Wang, and S. Trolier-McKinstry, "Links between defect chemistry, conduction, and lifetime in heavily Nb doped lead zirconate titanate films," Appl. Phys. Lett. **121**, 162903 (2022).
14) K. Coleman, M. Ritter, R. Bermejo, and S. Trolier-McKinstry, "Mechanical failure dependence on the electrical history of lead zirconate titanate thin films," J. Eur. Ceram. Soc. **41**, 2465 (2021).
15) K. Coleman, R. Bermejo, D. Leguillon, and S. Trolier-McKinstry, "Thickness dependence of crack initiation and propagation in piezoelectric microelectromechanical stacks," Acta Mater. **191**, 245 (2020).
16) C. Fragkiadakis, S. Sivaramakrishnan, T. Schmitz-Kempen, P. Mardilovich, and S. Trolier-McKinstry, "Heat Generation in PZT MEMS actuator arrays," Appl. Phys. Lett. **121**, 162906 (2022).
17) H. Kishi, Y. Mizuno, and H. Chazono, "Base-metal electrode-multilayer ceramic capacitors: past, present, and future perspectives," Jpn. J. Appl. Phys. **42**, 1 (2003).
18) F. Calame and P. Muralt, "Growth and properties of gradient free sol-gel lead zirconate titanate thin films," Appl. Phys. Lett. **90**, 062907 (2007).
19) J. Abergel, M. Allain, H. Michaud, M. Cueff, T. Ricart, C. Dieppedale, G. Le Rhun, D. Faralli, S. Fanget, and E. Defaÿ, "Optimized gradient free PZT thin films for micro-actuators," IEEE Int. Ultrason. Symp. **2012**, 972 (2012).
20) S. Pelloquin, G. LeRhun, E. Defaÿ, P. Renaux, E. Nolot, J. Abergel, and H. Sibuet, "Improvement of capacitive behavior on gradient free PZT thin films," Integr. Ferroelectr. **157**, 132 (2014).
21) T. Doi, T. Noguchi, J. Fujii, N. Soyama, and H. Sakurai, "The orientation and grain texture effect on life time reliability of sol-gel derived $PbZr_{0.52}Ti_{0.48}O_3$ films," Jpn. J. Appl. Phys. **51**, 09LA15 (2012).
22) T. Noguchi, H. Sakurai, J. Fujii, T. Doi, T. Watanabe, and N. Soyama, "Influence of film texture on reliability of sol-gel derived PZT thin-film capacitors," Key Eng. Mater. **566**, 7 (2013).
23) L. Pintilie, I. Vrejoiu, G. Le Rhun, and M. Alexe, "Short-circuit photocurrent in epitaxial lead zirconate-titanate thin films," J. Appl. Phys. **101**, 064109 (2007).
24) K. H. Hardtl and H. Rau, "PbO vapor pressure in the $Pb(Ti_{1-x}Zr_x)O_3$ system," Solid State Commun. **7**, 41 (1969).
25) Y. F. Zhukovskii, E. A. Kotomin, S. Piskunov, and D. E. Ellis, "A comparative ab initio study of bulk and surface oxygen vacancies in $PbTiO_3$, $PbZrO_3$, and $SrTiO_3$ perovskites," Solid State Commun. **149**, 1359 (2009).
26) T. M. Borman, W. Zhu, K. Wang, S. Won Ko, P. Mardilovich, and S. E. Trolier-McKinstry, "Effect of lead content on the performance of niobium-doped {001} textured lead zirconate titanate films," J. Am. Ceram. Soc. **100**, 3558 (2017).
27) J. Robertson and C. W. Chen, "Schottky barrier heights of tantalum oxide, barium strontium titanate, lead titanate, and strontium bismuth tantalate," Appl. Phys. Lett. **74**, 1168 (1999).
28) A. Klein, "Interface properties of dielectric oxides," J. Am. Ceram. Soc. **99**, 369 (2016).
29) J. Robertson, W. L. Warren, and B. A. Tuttle, "Band states and shallow hole traps in $Pb(Zr,Ti)O_3$ ferroelectrics," J. Appl. Phys. **77**, 3975 (1995).
30) M.-J. Pan, S.-E. Park, C. W. Park, K. A. Makowski, S. Yoshikawa, and C. A. Randall, "Superoxidation and electrochemical reactions during switching in $PbZrTiO_3$ ceramics," J. Am. Ceram. Soc. **79**, 2971 (1996).